

# Density functional calculations on small bimetallic magnetic clusters

S. Drenler<sup>1</sup>, J.L. Ricardo-Chavez<sup>2</sup>, J. Morillo<sup>1</sup>, and G.M. Pastor<sup>2,a</sup>

<sup>1</sup> Centre d'Élaboration de Matériaux et d'Études Structurales, CNRS, 31055 Toulouse, France

<sup>2</sup> Laboratoire de Physique Quantique, Université Paul Sabatier, CNRS, 31062 Toulouse, France

Received 10 September 2002

Published online 3 July 2003 – © EDP Sciences, Società Italiana di Fisica, Springer-Verlag 2003

**Abstract.** Structural and magnetic properties of small bimetallic clusters like  $\text{Co}_M\text{Rh}_N$ ,  $\text{NiNa}_N$ , and  $\text{NiCu}_N$  are determined in the framework of a generalized gradient-corrected approximation to density functional theory. The role of magnetism on the most stable structure and on the energy differences among the low-lying isomers is quantified by comparing magnetic and non-magnetic solutions of the Kohn-Sham equations. The correlation between structure, chemical order, and environment-dependent magnetic properties is discussed.

**PACS.** 36.40.Cg Electronic and magnetic properties of clusters – 75.75.+a Magnetic properties of nanostructures – 75.20.Hr Local moment in compounds and alloys; Kondo effect, valence fluctuations, heavy fermions

## 1 Introduction

The control of the size and composition of small clusters opens the way to a variety of new states of matter with physical and chemical properties that are often intrinsically different from those of conventional macroscopic crystals. A remarkably intense research activity is motivated by the resulting countless possibilities of generating novel materials with specifically tailored properties. Transition-metal (TM) clusters are particularly interesting in this context, since their magnetic properties are extremely sensitive to the local environment of the atoms and since magnetic nanostructures derived from them have multiple potential applications in recording and storage technologies. Previous studies have shown that the magnetic moments of  $\text{Fe}_N$ ,  $\text{Co}_N$ , and  $\text{Ni}_N$  clusters are significantly larger than the corresponding bulk magnetizations [1–7]. Moreover, non-vanishing magnetic moments have been observed in small clusters of some  $4d$  TM's, for example  $\text{Rh}_N$  with  $N \leq 50$ , which are non-magnetic in the solid state [8–10]. This enhancement of low-temperature magnetism in small particles can be qualitatively understood as a consequence of the reduction of local coordination number, which results in a stronger localization of the  $d$ -electron states and in a reduction of the effective  $d$ -band width. Notice, however, that the size dependence of the cluster structure and inter-atomic distances (typically 10–20% smaller than in bulk crystals) are also central to a precise determination of the ground-state moments. These are also known to affect profoundly other important

properties like the orbital moments, the stability of magnetism at finite temperatures, or the magnetic anisotropy energies per atom [11].

While numerous studies have been concerned with the magnetic properties of homonuclear clusters, very little is still known about alloy clusters or clusters containing magnetic impurities [12–14]. This is quite remarkable, since heterogeneous clusters are expected to show an extremely rich variety of magnetic behaviors as a function of composition and chemical order. For example, theoretical studies of  $(\text{Cr}_x\text{Fe}_{1-x})_N$  have revealed interesting transitions from ferromagnetic to antiferromagnetic-like order as a function of increasing Cr concentration  $x$ , which are accompanied by important changes in the average magnetic moments per atom [12]. Moreover, recent measurements have shown that bimetallic Co-Rh nanoparticles present average magnetizations per atom that are remarkably enhanced with respect to the macroscopic Co-Rh alloys of similar concentrations [13]. These systems are therefore good candidates for highly stable magnetic nanoparticles due to the stronger spin-orbit coupling at the  $4d$  atoms, a clear advantage for potential applications. On the other side, the behavior of magnetic impurities in simple or noble metal clusters deserves a special attention because of the many-body phenomena associated to valence fluctuations and dynamical magnetic screening [15,16]. In fact, recent theoretical studies of temperature-dependent electronic properties have revealed that metallic clusters containing magnetic impurities may show, under certain conditions, a Kondo-like screening of local magnetic moments which can be regarded as a finite-size equivalent of solid-state Kondo effect [14]. A systematic understanding of the

<sup>a</sup> e-mail: gustavo.pastor@irsamc.ups-tlse.fr

microscopic behavior of bimetallic clusters seems therefore most worthwhile.

The purpose of this paper is to report current investigations on structural and magnetic properties of Co-Rh alloy clusters and of Na and Cu clusters containing Ni impurities. First-principles calculations based on a generalized gradient approximation to density-functional theory (DFT) have been performed as briefly described in Section 2. Representative results for small clusters are presented and discussed in Sections 3 and 4. Finally, Section 5 points to some relevant future extensions.

## 2 Computational method

Electronic calculations involving transition-metal elements pose a considerable theoretical challenge due to the dominant role of valence  $d$ -electrons which are characterized by a relatively strong localization, directional bonding, and high density of states around the Fermi energy. The need for an accurate treatment of exchange-correlation effects, the presence of numerous close-lying electronic configurations with different spin multiplicities, and the possibility of multiple local minima in the configurational energy surface are additional problems that render *ab initio* studies on transition-metal clusters particularly difficult. The present work is based on DFT using a generalized gradient approximation (GGA) for exchange and correlation [17], which is currently one of the most widely used functionals in computational material science [18].

The calculations on  $\text{Co}_N\text{Rh}_M$  clusters have been performed by means of the Vienna *ab initio* simulation program (VASP) developed at the Institut für Materialphysik of the Universität Wien [19] which solves the spin-polarized self-consistent Kohn-Sham equations using a plane-wave basis set treating core-electron effects within the projector-augmented wave (PAW) approach [20]. The computational parameters such as plane-wave cut-off energy  $E_c$ , reciprocal lattice sampling, supercell size, etc. have been monitored in order to control the accuracy of the calculations. For isolated cluster calculations we use  $E_c = 14.7$  Ha and a supercell of about 10–15 Å, which ensures that the interactions between successive images are negligible. In this case only the  $\Gamma$  point of the Brillouin zone needs to be taken into account.

The results on  $\text{NiNa}_N$  and  $\text{NiCu}_N$  clusters have been obtained using the Amsterdam density-functional (ADF) program developed at the Vrije University, in which the Kohn-Sham orbitals are expanded in a basis of Slater-type orbitals (STO's) [21]. For the present study we considered the optimized set of triple-zeta STO's including polarization which is provided with the ADF package. All electronic states, including core states, have been taken into account explicitly in the self-consistent calculations. The reliability of the present choice of computational parameters (basis set, convergence criteria, etc.) has been checked by determining structural and electronic properties of  $\text{Na}_N$ ,  $\text{Cu}_N$ , and  $\text{Ni}_N$  homogeneous clusters and by

verifying that the results are in agreement with previous similar (DFT) studies.

The same GGA for exchange and correlation is used in all calculations [17]. For representative examples we have checked that the results obtained with the VASP and ADF codes coincide, which indicates that the results are consistent and reliable. All cluster structures have been optimized by relaxing fully the atomic positions without symmetry constraints until the forces  $\mathbf{F}_i$  on each atom  $i$  are vanishing (typically  $|F_i| \leq 0.01\text{--}0.02$  eV/Å). This is done for each relevant value of the  $z$  component of the total spin moment  $S_z$ . In this way the interplay between magnetism and ground-state structure is identified. Several different initial geometrical configurations corresponding to different cluster topologies are considered in order to detect nearby isomers. The structural and magnetic properties thus obtained are in good agreement with experiments and previous DFT studies on homogeneous clusters and periodic crystals.

## 3 $\text{Co}_N\text{Rh}_M$ clusters

In the case of dimers ( $N + M = 2$ ) the calculated interatomic bond length  $d$  are, as usual in small TM clusters, significantly smaller than in the corresponding solids. For  $\text{Rh}_2$ ,  $\text{CoRh}$ , and  $\text{Co}_2$  this contraction amounts to about 20% [22]. The trends in  $d$  for different compositions follow the results known for bulk materials where  $d_{\text{Co}} < d_{\text{CoRh}} < d_{\text{Rh}}$ . Concerning the dimer average magnetic moments, we find  $\bar{\mu}_N = 2\mu_B$  for all compositions. An interesting transfer of spin-density is observed in  $\text{CoRh}$ , where the integrated local moment  $\mu(i)$  around the Co atom is enhanced at the expense of the Rh moments. This can be qualitatively explained as a charge transfer from the  $4d$  Co orbitals to the  $5d$  Rh orbitals which allows the polarization of a larger number of Co  $d$  holes. The difference in the highest occupied Kohn-Sham eigenvalues for the isolated atoms ( $E_{\text{HOMO}}(\text{Co}) - E_{\text{HOMO}}(\text{Rh}) = 0.88$  eV) and their empirical Pauling electronegativities [ $\chi_P(\text{Co}) = 1.88$  and  $\chi_P(\text{Rh}) = 2.28$ ] are consistent with this interpretation. Similar effects are sometimes observed in larger clusters.

Results for  $\text{Co}_M\text{Rh}_N$  with  $N + M = 4$  atoms are presented in Figure 1. One observes a monotonous decrease of the cohesive energy as we go from the pure  $\text{Rh}_N$  to pure  $\text{Co}_N$ , in agreement with the lower cohesive energy of bulk Co compared to bulk Rh. The most stable structure are in general three dimensional ( $N \geq 4$ ) with planar isomers found at nearby energies. All studied  $\text{CoRh}$  clusters are magnetic with average spin moment per atom  $\bar{\mu}$  and local spin moments  $\mu(i)$  that are often a factor 2 larger than those of macroscopic crystals or alloys with similar concentrations. Moreover, one observes that  $\bar{\mu}$  and  $\mu(i)$  tend to increase with increasing fraction of Co atoms. In some cases, the replacement of just one Rh atom by Co can lead to a remarkable global spin polarization and enhancement of the total cluster moment, which goes well beyond the individual contribution of the replaced atom.

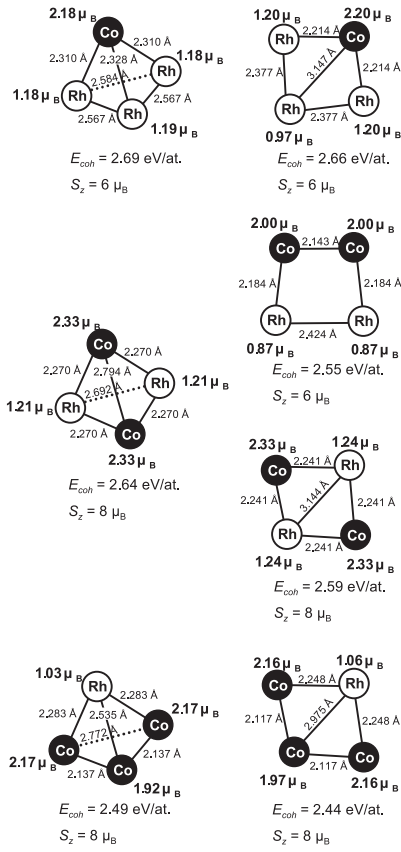


**Fig. 1.** Magnetic and structural properties of  $\text{Co}_M\text{Rh}_N$  clusters having  $N + M = 4$  atoms: cohesive energy per atom  $E_{coh}$ , nearest-neighbor bond-lengths,  $z$  component  $S_z$  of the total spin moment, and local spin moments  $\mu(i)$  at each atom  $i$ .

From a local point of view one observes that the magnetic moments at Co atoms [typically  $\mu(\text{Co}) \simeq 2\mu_B$ ] are not significantly affected by the Rh concentration even if the latter is increased beyond 50%. The presence of Rh does not reduce the Co moments, as one might have expected. In some cases even a slight enhancement is found. This behavior contrasts with the important reduction of Co moments observed in some macroscopic Co-Rh alloys, and can be a consequence of the extremely reduced coordination number in these small clusters. From the point of view of Rh, the presence of Co atoms in the cluster results in a remarkable increase of the local moments and in a larger stability of magnetism. This is particularly noticeable in the case of tetrahedral  $\text{Rh}_3\text{Co}$  where the enhancement of  $\mu_{\text{Rh}}(i)$  reaches more than  $1\mu_B$ .

The results for  $\text{Co}_2\text{Rh}_2$  illustrate the influence of other effects, such as isomerization and segregation, on the total magnetization. Comparing the two planar geometries, one finds that the structure where the Co atoms are separated by a strongly bonded  $\text{Rh}_2$  dimer exhibits a significantly enhanced total magnetic moment ( $\Delta S_z = 2\mu_B$ ). This is due to an enhancement of the local moments at both Co and Rh atoms. Note that this structure is somewhat more stable ( $\Delta E = 0.04$  eV/atom) than the planar one having

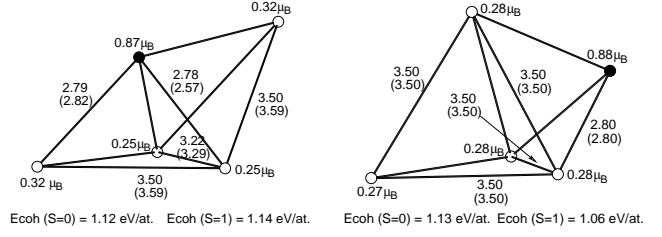


**Fig. 2.** Electronic and structural properties of the calculated isomers of  $\text{NiNa}_4$ : cohesive energy per atom  $E_{coh}$ , nearest neighbor bond-lengths (in Å), and local magnetic moments  $\mu(i)$  in the magnetic solution having  $z$  component of the total spin  $S_z = 1$ . The values in brackets refer to the non-magnetic solution. Filled (open) circles indicate Ni (Na) atoms.

$S_z = 6\mu_B$ , but less stable than the tetrahedron ( $\Delta E = 0.05$  eV/atom).

The role of magnetism on the equilibrium structures and on the energy differences among the lowest isomers can be identified by comparing magnetic and non-magnetic calculations. The stabilization energy due to magnetism can reach 0.5 eV/atom. It increases with the proportion of Co atoms and with increasing magnitude of the local magnetic moments. In the case of  $\text{Co}_M\text{Rh}_N$  with  $N + M \leq 4$  the relative stability among the isomers does not appear to be changed when magnetism is not taken into account in the calculations. However, an important bond-length contraction of about 5% is observed in non-magnetic equilibrium structures as compared to the magnetic ones. This can be qualitatively understood in terms of the single-particle spectrum, since the spin polarization requires the promotion of electrons from bonding to anti-bonding or less bonding  $d$  states.

## 4 $\text{NiNa}_N$ and $\text{NiCu}_N$ clusters

In Figure 2 results are given for the geometry of the equilibrium isomers, cohesive energies per atom  $E_{coh}$ , nearest neighbor bond-lengths, and local magnetic moments  $\mu(i)$  of  $\text{NiNa}_4$ . These are representative of a much larger set of calculations performed for  $\text{NiNa}_N$  and  $\text{NiCu}_N$  with  $N \leq 6$ . Both magnetic ( $S_z \geq 1$ ) and non-magnetic calculations have been performed. Among the former, only the case  $S_z = 1$  needs to be considered in the following, since the  $S_z \geq 2$  states are far less stable. The equilibrium structures of small  $\text{NiNa}_N$  and  $\text{NiCu}_N$  clusters can be regarded either as a distorted  $\text{Na}_N$  or  $\text{Cu}_N$  with an adsorbed Ni atom, or as a distorted  $\text{Na}_{N+1}$  or  $\text{Cu}_{N+1}$  with one of the non-magnetic metal atoms replaced by a Ni. In both cases the distortions resulting from the presence of the Ni impurity are important. They are driven by the tendency to shorten the Ni-Na or Ni-Cu bonds (see Fig. 2). Typically, Na-Na (Cu-Cu) bond lengths are about 3.0–3.6 Å (2.4–2.5 Å), *i.e.*, similar to those of pure Na (Cu) clusters. The Ni-Na (Ni-Cu) bond lengths are shorter, in range of 2.6–2.9 Å (2.3–2.5 Å). Comparing magnetic and non-magnetic geometry optimizations we observe that Na-Na and Cu-Cu bonds are in general slightly larger in the

non-magnetic case (by about 0.1–0.2 Å), while the Ni-Na and Ni-Cu bonds are shorter (by about 0.1–0.2 Å). However, no simple trends can be inferred concerning the role of magnetism on the relative stability of different cluster topologies or different impurity positions within the cluster. For some clusters, as shown for example in Figure 2, the ordering of magnetic and non-magnetic solutions is reversed in different isomers. In other cases the most stable geometry is not qualitatively affected by the magnetic effects. In any case, single-triplet gaps and isomerization energies are comparable. Therefore, spin excitations and structural changes are likely to coexist at low temperatures. A similar situation has been found in previous model calculations [14].

Concerning the spin-density distribution and electronic configurations of the atoms, we observe that charge transfers between the impurity and Na or Cu host atoms are small. Typically, 0.1–0.2 electrons are transferred to the Ni impurity. In all considered clusters the number of  $d$  electrons at the Ni atom is close to  $n_d = 9$  ( $n_d = 8.9$ – $9.1$  in the  $S_z = 1$  solution, and  $n_d \simeq 9.2$  in the non-magnetic case). Moreover, the Ni  $d$ -holes are almost fully polarized in the  $S_z = 1$  ground state [ $\mu(\text{Ni}) \simeq 1\mu_B$ ]. In this case, non-negligible magnetic moments are also induced in the metallic host [typically,  $\mu(\text{Na}) = 0.1$ – $0.3\mu_B$ ] which align parallel to the Ni moment ( $S_z = 1$ , see Fig. 2). The local moment formation criterion being satisfied [15, 16], an interesting spectrum of low-energy spin excitations may be expected in these clusters [14].

## 5 Discussion

Small CoRh clusters are magnetic with average moments per atom that are significantly larger than those of bulk alloys of similar concentrations. Our results are consistent with experiments on nanometer-scale Co-Rh particles [13]. However, it is still unclear at present to what extent these trends are specific to the very small sizes considered here. In fact, for  $M+N \leq 4$  atoms the local coordination numbers are so small that the finite-size effects and the reduction of effective  $d$  band width should largely dominate over the Co-Rh hybridizations. Another question of considerable interest for these experiments concerns the chemical ordering and the possible role of segregation on the magnetic behavior. The present calculations show that the energy differences between isomers are relatively small. Therefore, the coexistence of different chemical orderings, often showing different magnetic properties, cannot be excluded. Calculations on larger clusters allowing a greater diversity of chemical and structural orderings and the comparison between measured and calculated magnetic properties should allow to infer complementary structural information.

The DFT calculations on metallic clusters containing magnetic impurities have revealed a rich variety of nearby lying low-energy isomers with important reorganizations of bond lengths that reflect strong simple-metal to transition-metal binding. Concerning the electronic configurations, a clear and systematic indication is provided

that a Ni impurity in  $\text{Na}_N$  or  $\text{Cu}_N$  is close to a  $d^9s^1$  state. This implies that Ni should preserve its magnetic  $d$ -hole degree of freedom. However, at the present stage no reliable information can be inferred on the nature of the magnetic coupling between this local spin and the delocalized  $sp$ -electrons. This is due, at least in part, to the impossibility of treating well-defined total spin states (singlet and triplet states, for example) with the available exchange and correlation functionals. Correlated calculations are required that take explicitly into account the relevant  $d$  electron configurations and their coupling to  $sp$  levels around the Fermi energy. Research in this direction is currently in progress.

This work was financed in part by the EU GROWTH project AMMARE (G5RD-CT-2001-00478). Computer resources were provided by IDRIS and CALMIP (France). One of the authors (JLRC) acknowledges support from CONACyT (Mexico).

## References

1. I.M.L. Billas *et al.*, *Science* **265**, 1682 (1994); S.E. Apsel *et al.*, *Phys. Rev. Lett.* **76**, 1441 (1996)
2. M. Respaud *et al.*, *Phys. Rev. B* **59**, R3934 (1999)
3. K. Lee *et al.*, *Phys. Rev. B* **30**, 1724 (1985); *ibid.* **31**, 1796 (1985); G.M. Pastor *et al.*, *ibid.* **40**, 7642 (1989)
4. C. Jamorski *et al.*, *Phys. Rev. B* **55**, 16 (1997); M. Pereira *et al.*, *Int. J. Quant. Chem.* **81**, 422 (2001)
5. Y. Jinlong *et al.*, *Phys. Rev. B* **50**, 11 (1994); C.H. Chien *et al.*, *Phys. Rev. A* **58**, 3 (1998)
6. M. Castro *et al.*, *Chem. Phys. Lett.* **271**, 133 (1997); B.V. Reddy *et al.*, *J. Phys. Chem. A* **102**, 1748 (1998); F.A. Reuse, S. Khanna, *Eur. Phys. J. D* **6**, 77 (1999)
7. G.M. Pastor, in *Atomic clusters and nanoparticles*, edited by C. Guet *et al.* (EDP Sciences, Les Ulis, Springer, Berlin, 2001), p. 335ff
8. A.J. Cox *et al.*, *Phys. Rev. Lett.* **71**, 923 (1993); *Phys. Rev. B* **49**, 12295 (1994)
9. B.V. Reddy *et al.*, *Phys. Rev. Lett.* **70**, 3323 (1993)
10. P. Villaseñor-González *et al.*, *Phys. Rev. B* **55**, 15084 (1997)
11. G.M. Pastor *et al.*, *Phys. Rev. Lett.* **75**, 326 (1995)
12. A. Vega *et al.*, *Z. Phys. D* **19**, 263 (1991)
13. D. Zitoun *et al.*, *Phys. Rev. Lett.* **89**, 037203 (2002)
14. J.L. Ricardo-Chávez, G.M. Pastor, *J. Appl. Phys.* **87**, 6800 (2000); *Eur. Phys. J. D* **16**, 169 (2001)
15. P.W. Anderson, *Phys. Rev.* **124**, 41 (1961)
16. C.M. Varma, Y. Yafet, *Phys. Rev. B* **13**, 2950 (1976)
17. J.P. Perdew *et al.*, *Phys. Rev. B* **46**, 6671 (1992)
18. For a review on DFT as a computational tool in cluster physics see, for instance, S. Chrétien, D.R. Salahub, in *Atomic clusters and nanoparticles*, edited by C. Guet *et al.* (EDP Sciences, Les Ulis, Springer, Berlin, 2001), p. 107ff
19. G. Kresse, J. Hafner, *Phys. Rev. B* **47**, 558 (1993); G. Kresse, J. Furthmüller, *ibid.* **54**, 11169 (1996)
20. P.E. Blöchl, *Phys. Rev. B* **50**, 24 (1994)
21. ADF 2002, Theoretical Chemistry, Vrije Universiteit Amsterdam: E.J. Baerends *et al.*, *Chem. Phys.* **2**, 41 (1973); G. Velde, E.J. Baerends, *Comp. Phys.* **99**, 84 (1992)
22. H. Wang *et al.*, *J. Chem. Phys.* **106**, 2101 (1997)